drones

MDPI

Article

Drop Nozzle from a Remotely Piloted Aerial Application System Reduces Spray Displacement

Ryan P. Gibson [1], Daniel E. Martin [2,*], Zachary S. Howard [1], Scott A. Nolte [1] and Mohamed A. Latheef [2]

[1] AgriLife Extension, Department of Soil and Crop Sciences, Texas A&M University, College Station, TX 77843, USA; rpgibson45@tamu.edu (R.P.G.); zachary.howard@ag.tamu.edu (Z.S.H.); scott.nolte@ag.tamu.edu (S.A.N.)
[2] Aerial Application Technology Research Unit, United States Department of Agriculture, College Station, TX 77845, USA; mohamed.latheef@usda.gov
* Correspondence: dan.martin@usda.gov

Abstract: Weeds remain one of the major limiting factors affecting agricultural production, causin significant yield loss globally. Spot spraying of resistant weeds as an alternative to broadcast applications provides the delivery of chemicals closer to the plant canopy. Also, wind speed can cause spray displacement and can lead to inefficient coverage and environmental contamination. To mitigate this issue, this study sought to evaluate drop nozzles configured to direct the spray closer to the target. A remotely piloted aerial application system was retrofitted with a 60 cm drop nozzle comprising a straight stream and a 30° full cone nozzle. A tracer spray solution was applied on 13 Kromekote cards placed in a grid configuration. The center of deposition for each spray application was determined using the Python (3.11) software. Regardless of nozzle angle, the drop nozzle produced ca. 76% lower spray displacement than the no drop nozzle. The no drop nozzles had a narrower relative span compared to the drop nozzles. This suggests that smaller, more driftable fractions of the spray did not deposit on the targets due to spray displacement. Additional research investigating in-field weed species under various meteorological conditions is required to move this technology forward.

Keywords: precision agriculture; drop nozzle; spray displacement; straight stream nozzle; nozzle angle

Academic Editor: Pablo Rodríguez-Gonzálvez

Received: 14 December 2024
Revised: 23 January 2025
Accepted: 28 January 2025
Published: 6 February 2025

Citation: Gibson, R.P.; Martin, D.E.; Howard, Z.S.; Nolte, S.A.; Latheef, M.A. Drop Nozzle from a Remotely Piloted Aerial Application System Reduces Spray Displacement. *Drones* **2025**, *9*, 120. https://doi.org/10.3390/drones9020120

1. Introduction

Weeds are one of the major limiting factors in the production of agricultural crops, causing significant yield loss in crop farming systems throughout the world. It is estimated that weeds in corn and soybean alone would reduce yield by 50%, costing growers USA $43 billion in economic loss annually in the United States and Canada according to a study conducted over a seven-year period [1]. When a pre-emergence herbicide was used, surviving weeds began to reduce corn yields after about 6 weeks, with grasses having greater effect than broadleaf weeds [2]. Early germinating weeds reduce yield more than weeds which emerge later in the growing season [3]. Most importantly, recent events due to climate change have precipitated an increased concentration of CO_2 in the atmosphere, which can influence the efficacy of herbicides and weed management. The C_3 weeds would be able to develop resistance to glyphosate, a non-selective, post-emergent widely used herbicide, more easily than C_4 weeds under increased concentration of CO_2 [4–6].

The cost of weed control in North American farmlands remains high; therefore, controlling weeds efficiently is imperative for reducing farmers' overhead costs and increasing

farm productivity [7]. The conventional approach for controlling weeds in production agriculture has relied on broadcast applications of herbicides across the entire field. This approach has brought in its wake environmental concerns and a concomitant resurgence of resistant weeds. Spot spraying of weeds as an alternative method is commensurate with the spatial distribution of weeds since they often occur in patches within crop fields [8,9]. Using geostatistics, Johnson et al. [8] reported that inherent variability of seed dispersal, germination, seed and seedling mortality events primarily contribute to the patchy distribution of weed populations. Besides weeds, arthropod pest outbreaks in production in agriculture often occur as a clumped or contagious skewed spatial pattern. For instance, cabbage aphids in canola fields, and Asian psyllids in citrus orchards occur in their highest population densities along field edges [10–12]. Aphids on soybean and two-spotted spider mites on cowpea occur when exposed to abiotic stress, such as drought or nutrient deficiencies tend to be more susceptible [13–15]. Thus, as pests occur as spatially aggregated and heterogeneous cohorts, precision technology can offer opportunities for controlling these organisms without unduly affecting the environment [16].

The integration of drone technology or remotely piloted aerial application systems (RPAASs) into farming practices is a significant advancement in crop management, particularly in the application of pesticides and herbicides. One of the primary challenges in this domain is the displacement of spray caused by wind and rotor wash, which can lead to inefficient coverage and deleterious effects on the environment. To mitigate this issue, drop nozzles have been developed which extend below the main body of the drone, enabling the delivery of chemicals closer to the crop canopy and reducing the distance the spray must travel before reaching the target. This design minimizes the likelihood of spray drift, as it decreases exposure to wind shear and enables more direct spray application. Moreover, drop nozzles provide improved canopy penetration, ensuring better coverage of weeds and pests, particularly in dense or tall cropping systems.

The RPAAS platforms utilize advanced sensors and algorithms for on-line weed detection using digital image analysis, computer-based decision making and GPS-controlled patch spraying [17,18]. This helps identify and treat specific areas infested with weeds, minimizing the use of chemicals and promoting sustainable agricultural practices. Hunter III et al. [19] reported that the UAVs are more efficient in identifying and treating targeted weedy areas, while minimizing treatment on non-weedy areas, compared to ground-based broadcast applications. Several researchers have reported that hyperspectral imaging sensors mounted on RPAAS systems detected weeds at the early stage of weed growth by flying at low application heights and taking ultra-high spatial resolution imagery and observed dispersion of small weeds [17,20,21]. Allmendinger et al. [22] achieved up to 86% efficacy and saved 47% on herbicide cost using a high-resolution UAV camera mounted on a tractor and reported that early spot spraying greatly improved herbicide efficacy compared to broadcast treatments, and significantly reduced herbicide use. Using a RPAAS system, Richardson et al. [23] developed and quantified a method for spot spraying invasive conifer trees with crown diameters in the range of 1 to 2 m in New Zealand forests. Singh et al. [24] discussed the challenges facing the UAS-based remote sensing technologies including hardware engineering, platform navigation capabilities, sensor miniaturization, sensor integration and payload problems, and data acquisition strategies. Image preprocessing poses unique challenges with respect to the accuracy associated with radiometric calibration, geometric correction, and image mosaicking [24]. Roslim et al. [25] reported that the integration of drones, artificial intelligence, and various sensors, which include hyperspectral, multi-spectral, and RGB (red–green–blue) would help in ensuring weed management sustainability by accurately identifying weed patches in cultivated fields. Ghatrehsamani et al. [26] reported that adding mechanical arms, laser, or electrocution

in the AI-based detection systems would help overcome the resistant weed management. Carbon dioxide lasers and electrocution have also been reported to annihilate weeds in large acre farms, as resistant weeds continue to evolve as a major impediment for increased farm productivity [27,28].

These reports highlight the need for technologically advanced techniques inclusive of remote sensing and AI innovations for the detection of resistant weeds in farmscapes. However, very little information exists on a RPAAS platform configured to spot treat individual resistant weeds among a hodgepodge of heterogeneous weed patches in production agriculture. This study describes a retrofitted nozzle system configured for such use on a RPAAS platform and evaluates its efficacy on an artificial target established to capture spray deposits and to assess spray displacement.

Objectives of this study were to evaluate the role of drop nozzles for increasing spray accuracy by reducing the effect of wind speed on spray displacement. Specifically, we wanted to determine the effect of drop nozzles on spray displacement vis-à-vis wind speed which is a major impediment to targeted applications.

2. Materials and Methods

This study was conducted in an unpaved area surfaced with gravel in Burleson County, near College Station, TX, USA (30°40′ N, 96°18′ W). The targeted spray location comprised 13 wooden blocks established in a grid where the number 7 was the center target card, which served as the cynosure of spray deposition (Figure 1). These wooden blocks (10 cm × 10 cm) were arranged with 0.31 m spacing between each other. A paper clip was attached to each of the blocks with a sheet metal screw. An 89 mm × 89 mm Kromekote card (CTI Paper USA, Neenah, WI, USA) was placed into each paper clip. The RPAAS used was a six rotor, sixteen-liter Precision Vision 35X (PV35X, Leading Edge Aerial Technologies, New Smyrna Beach, FL, USA) (Figure 2). It has a custom single spot-spray nozzle mounted directly underneath the fuselage (Figure 3). Figure 4 is the schematic description of the spray nozzle configuration showing rotors, arms, and a single spot spray nozzle. The RPAAS was equipped with an RTK guidance system (Herelink 2, Hex Technology, Austin, TX, USA) while spraying to provide centimeter level accuracy to hit the center target card (card 7) on the grid. Four nozzle configurations; (1) 30° with a 60 cm drop (30D), (2) 30° with no drop (30ND), (3) straight stream with 60 cm drop (SSD), and (4) straight stream with no drop (SSND) were used. The drop nozzle allows for a more stable spray application in high wind situations.

The drop nozzle consists of four components, all of which are commercially available. The main component is a 60 cm braided steel dishwasher hose (BrassCraft, Novi, MI, USA). The side of the hose connected to the drone was a standard female TEEJET QJ1/4T-NYB (TeeJet, Glendale Heights, IL, USA) quick connect fitting. For the lower part of the hose a male TEEJET QJ1/4TT-NYB (TeeJet, Glendale Heights, IL, USA) quick connect fitting was used to allow common nozzle caps to be used with the drop nozzle. To reduce the effect of wind on the nozzle, ten washers were placed around the hose to add weight to the nozzle end of the hose (Figure 5). The major difference in a conventional drop nozzle used on a ground rig application compared to a drone mounted drop nozzle is the need for a flexible hose in drone applications to allow for landing without damaging spray components. Many standard types of drop nozzles are a solid tube or semi flexible, but only to the point of not breaking if a stalk is struck by the nozzle. The flexible hose prevents any damage from occurring due to striking an object and landing the drone with no special equipment or platform.

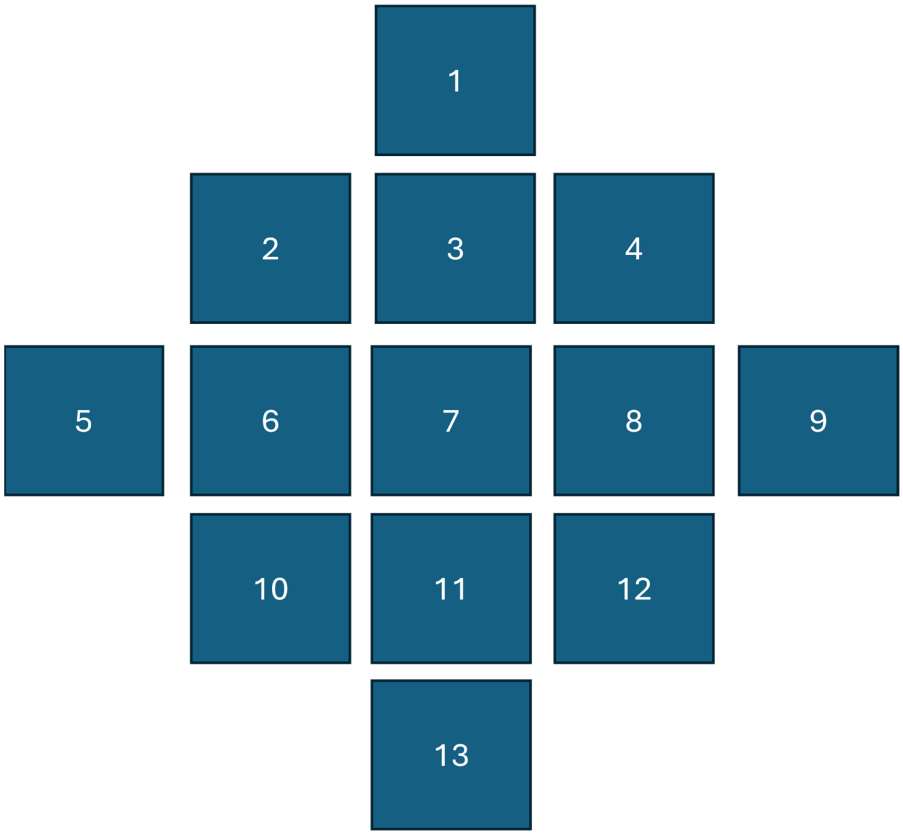

Figure 1. Layout of the test area where artificial samplers (Kromekote cards) were placed in a grid fashion for sampling spray deposits. The number on the card is the labeling system used to track the location of each card. The center card #7 served as the cynosure of deposition from where the spray displacement was calculated.

Figure 2. Spray drone outfitted with spot spray drop-nozzle hovering over the center of the targeted area.

Figure 3. Spray drone outfitted with a conventional spot spray nozzle.

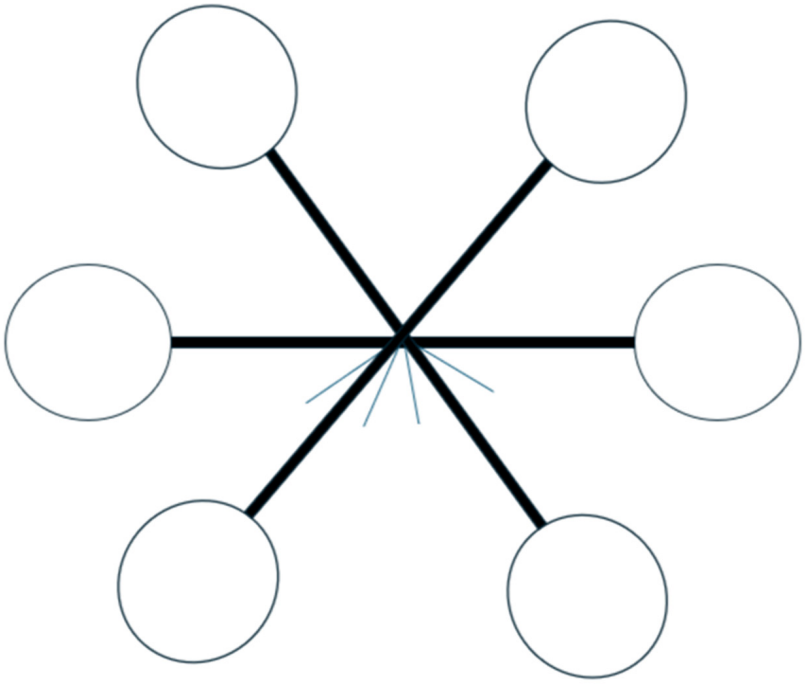

Figure 4. Spray drone configuration showing rotors, arms, and single spot spray nozzle placement. Blue lines represents spray from the nozzle.

The spray solution comprising water plus Rhodamine dye mixed at 20 mL/L was sprayed on Kromekote cards as shown in Figure 1. The treatments used in this study were described in Table 1.

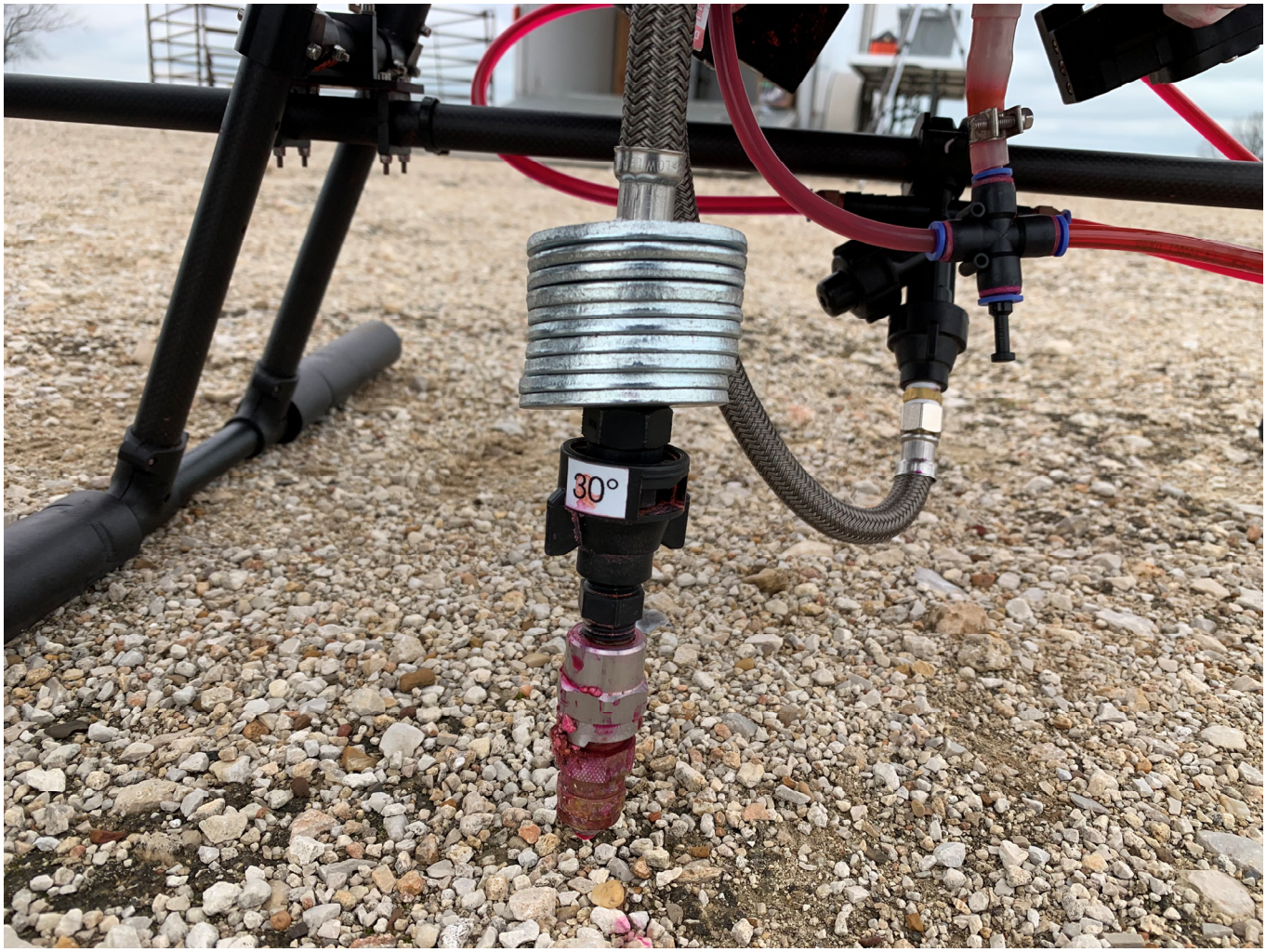

Figure 5. Spot spraying nozzle (30°) with drop tube and washers.

Table 1. Descriptions of treatments used in the study.

Treatment	Angle	Drop	Replication
1	0	No Drop	1
1	0	No Drop	2
1	0	No Drop	3
1	0	No Drop	4
1	0	No Drop	5
2	0	Drop	1
2	0	Drop	2
2	0	Drop	3
2	0	Drop	4
2	0	Drop	5
3	30	No Drop	1
3	30	No Drop	2
3	30	No Drop	3
3	30	No Drop	4
3	30	No Drop	5
4	30	Drop	1
4	30	Drop	2
4	30	Drop	3
4	30	Drop	4
4	30	Drop	5

2.1. Take-Off and Landing with the Drop Nozzle

When equipped with the drop nozzle, a special landing technique needs to be used to prevent damage to the nozzle and/or drone. The pilot needs to hover the drone with the nozzle just above the ground. Once the pilot is ready to land the aircraft, the pilot needs to slowly lower the aircraft to the ground. When the nozzle first touches the ground, the pilot then continues to lower the aircraft while backing the aircraft up until the drone is completely landed. This prevents any damage to the nozzle or the aircraft.

2.2. Determination of Spray Displacement

Once the RPAAS had the coordinates of the center card, it was moved to the takeoff location. For all treatments, the RPAAS hovered at 1.52 m over the target area. For the no drop nozzle treatments, the nozzle height was equal to the RPAAS height. For the drop nozzle treatments, the nozzle height was 0.92 m over the target area. The pump pressure was set at 345 Kpa (50 psi). The RPAAS was programmed to hover over the target area for 5 s to stabilize its x, y, and z (latitude, longitude, and height) position and the nozzle prior to the spray application. The spray was released for 1 s which provided a dose of 30 mL (1 oz). The Kromekote cards were left for 3–5 min to dry on the wooden blocks before being moved to a table and then transported to the laboratory for processing. Wind speed, wind direction, and temperature were measured during each spray application (Tables 2 and 3). The weather conditions during the study were variable, with wind speed being the major determinant that influenced spray displacement. For the 0° angle drop nozzle treatment, the wind speed varied from 5 to 9 m/s, while for 30° angle drop nozzle treatment, the wind speed varied from 2 to 7 m/s. This indicates that the wind speed during the test was not evenly distributed for the 0° and 30° angle tests and thus, it remains a limiting factor in this study.

Table 2. Meteorological conditions during the test period using straight stream nozzles (0°).

Meteorological Parameter	No Drop Nozzle					Drop Nozzle				
	R1	R2	R3	R4	R5	R1	R2	R3	R4	R5
Wind Speed (m/s)	6.7	6.7	6.7	7.6	7.2	5.4	4.9	5.4	8.9	7.6
Wind Direction	N	N	N	N	N	N	N	N	N	N
Temp (°C)	17.2	17.2	17.2	17.8	17.2	16.1	16.1	16.1	16.1	16.1

Table 3. Meteorological conditions during the test period using straight stream nozzles (30°).

Meteorological Parameter	No Drop Nozzle					Drop Nozzle				
	R1	R2	R3	R4	R5	R1	R2	R3	R4	R5
Wind Speed (m/s)	3.6	3.6	5.8	4.5	5.4	7.2	2.2	4.5	2.7	6.3
Wind Direction	S	S	S	S	N	N	S	S	S	N
Temp (°C)	27.8	29.4	30.0	30.0	17.8	17.2	27.8	27.8	27.8	17.2

A coordinate point was assigned to every Kromekote card on the grid. Python software [29] was used to generate a heat map showing the % area coverage for each treatment. Two libraries, NumPy and pandas, were used to analyze the data and convert them into data that could be used by the graphic design library matplotlib. Pandas performs data preparation in the form of tables and spreadsheets, while NumPy used the numerical computation of the data. The program used sigmoid interpolation to better represent the % area coverage. The centroid was calculated using Python software to identify the center of spray deposition (Figure 6).

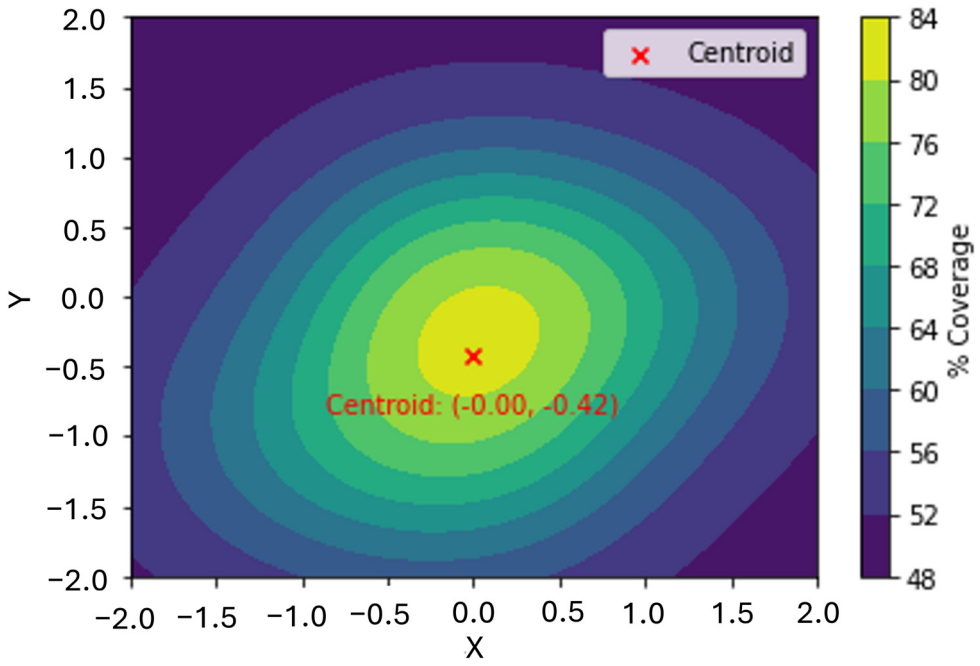

Figure 6. Topographic heat map showing spray deposition and center of deposition (centroid). The X and Y axis on the grid represent a cartesian coordinate. A card was placed at every whole number which was spaced 0.3 m apart. This figure is an interpolated representation of the data collected from Figure 1.

2.3. Determination of Spray Droplet Characteristics

The Kromekote cards were analyzed using the AccuStain software (0.35) (University of Illinois at Urbana-Champaign, Urbana-Champaign, IL, USA). A representative sample of these analyzed cards is shown in Figure 7. The cards were placed in order, from top to bottom of the grid (Figure 1). The spray droplet spectra measured were $D_{v0.1}$, $D_{v0.5}$, $D_{v0.9}$, percent area coverage, and relative span (RS). $D_{v0.1}$ is the droplet diameter (µm) where 10% of the spray volume is contained in droplets smaller than this value. Similarly, $D_{v0.5}$ and $D_{v0.9}$ are droplet diameters where 50% and 90% of the spray volumes are contained in droplets smaller than these values, respectively. $D_{v0.5}$ is commonly known as the volume median diameter (VMD). RS is a dimensionless parameter and measures the width of the droplet spectra around $D_{v0.5}$, describing the uniformity of the drop size distribution and is calculated as:

$$RS = (D_{v0.9} - D_{v0.1})/D_{v0.5}. \quad (1)$$

The American Society of Agricultural and Biological Engineering has developed the ASABE S572.3 Droplet Size Classification, a standard to measure and interpret spray quality tips for aerial application spray nozzles [30]. The VMD of the spray droplet sizes that were released from the spray tips in this study comprised fine (106–235 µm), medium (236–340 µm), coarse (341–403 µm), very coarse (404–502 µm), and extra coarse (503–760 µm) spray droplet spectra.

All statistical analyses of the data were conducted using the JMP® software (https://www.jmp.com/en_us/home.html, accessed on 27 January 2025) [31]. The assumption of homogeneity of variance is a prerequisite while conducting ANOVA and to obtain reliable results [32]. To test the equality of variance of the data, the drop and no drop nozzle data were pooled, and were then sorted by 0°and 30° angles. Levene's test was performed for each of the spray droplet spectra from 0°and 30° angles to test the null hypothesis that the variances were equal (Table 4). The results of the analysis indicated that although some of the droplet parameter data did represent unequal variance, most of the data (58%) were

homoscedastic. Therefore, the analysis of variance of the spray droplet data was conducted without transformation. The analysis of means, (ANOM) which is an alternative to one-way analysis of variance (ANOVA) for a fixed effects model, was used to compare the slopes between drop and no drop nozzles and those between nozzles set at 0° and 30° [33]. Unlike ANOVA, which simply determines whether there is a statistically significant difference between treatment means, ANOM identifies the means that are significantly different from the overall mean.

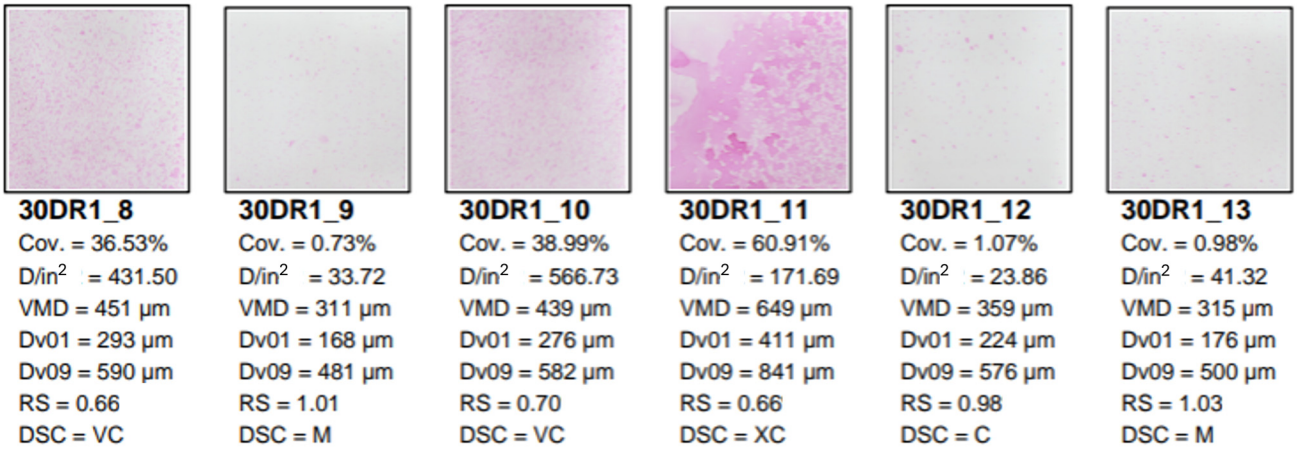

Figure 7. Representative sample of Kromekote cards with rhodamine dye deposits, describing droplet spectra from a field study analyzed with AccuStain software.

Table 4. Analysis of spray droplet parameters to test homogeneity of variance using Levene's Test.

Droplet Parameter	0°			30°		
	F	***p***	**Df ***	***F***	***p***	**Df**
% Coverage	5.24	0.02	1, 117	0.27	0.60	1, 117
Droplet Density	5.24	0.02	1, 108	0.27	0.60	1, 117
$D_{v0.1}$	6.57	0.01	1, 107	7.46	0.0073	1, 111
$D_{v0.5}$	1.65	0.20	1, 107	3.87	0.05	1, 111
$D_{v0.9}$	5.09	0.03	1, 107	0.34	0.56	1, 111
Relative Span	2.56	0.11	1, 107	0.39	0.53	1, 111

* Degrees of freedom.

3. Results

3.1. Spray Droplet Spectra

The spray droplet characteristics determined for the treatments used in this study are presented in Table 5. Regardless of nozzle angle, there was no significant difference in percent area coverage or droplet density between the drop and no drop nozzle. The $D_{v0.1}$ spray droplets differed significantly between the drop and no drop nozzles for the 30° nozzle but not for the 0° nozzle. The no drop nozzle produced larger $D_{v0.1}$ droplets than the drop nozzle. This suggests that with the drop nozzle being closer to the target, most of the smaller droplets reached the target instead being blown away by the wind. For VMD, the trend was similar to that of the $D_{v0.1}$ spray droplets. The $D_{v0.9}$ droplets were not significantly different between the drop and no drop nozzles, regardless of nozzle angle. However, the RS which measures the width of the droplet spectra around $D_{v0.5}$ droplets (Equation (1)), varied significantly between drop and no drop nozzles for both 0° and 30° nozzles. The no drop nozzles had a narrower RS compared to the drop nozzles. A plausible explanation for this effect may be that the smaller, more driftable fractions of the spray were

not able to deposit on the targets due to spray displacement from the wind. This would reduce the RS which is based on the difference between $D_{v0.9}$ and $D_{v0.1}$ divided by $D_{v0.5}$. When the smaller droplet fraction is blown away from the target, the $D_{v0.1}$ value increases, thus making the difference between $D_{v0.9}$ and $D_{v0.1}$ smaller, which reduces the RS.

Table 5. Spray droplet characteristics for the spray deposits on artificial collectors using straight stream and 30° full cone drop nozzles.

Nozzle	0°				30°			
	% Area Coverage ($\bar{x} \pm$ SEM) *				% Area Coverage ($\bar{x} \pm$ SEM)			
	Mean	*F*	*p*	Df	Mean	*F*	*p*	Df
Drop	11.60 ± 2.50 a	0.47	0.49	1, 80.7	28.13 ± 4.38 a	0.17	0.68	1, 115.2
No Drop	14.82 ± 3.94 a				30.76 ± 4.67 a			
	Droplet Density (Drops/cm^2)				Droplet Density (Drops/cm^2)			
Drop	74.87 ± 16.13 a	0.52	0.47	1, 108	181.50 ± 28.18 a	0.17	0.68	1, 117
No Drop	95.59 ± 25.44 a				198.47 ± 30.11 a			
	$Dv_{0.1}$, µm				$Dv_{0.1}$, µm			
Drop	248.47 ± 6.43 a	0.04	0.85	1, 107	254.57 ± 16.52 b	9.64	0.002	1, 111
No Drop	246.11 ± 11.56 a				342.66 ± 24.11 a			
	$D_{v0.5}$, µm				$D_{v0.5}$, µm			
Drop	448.40 ± 12.44 a	0.31	0.58	1, 107	448.24 ± 25.93 b	8.86	0.0036	1, 111
No Drop	437.36 ± 15.76 a				574.10 ± 34.42 a			
	$D_{v0.9,}$ µm				$D_{v0.9,}$ µm			
Drop	628.53 ± 15.39 a	2.83	0.09	1, 107	616.59 ± 28.13 a	3.88	0.05	1, 111
No Drop	582.87 ± 23.65 a				703.64 ± 34.74 a			
	Relative Span				Relative Span			
Drop	0.85 ± 0.02 a	5.19	0.02	1, 107	0.87 ± 0.03 a	17.13	0.0001	1, 111
No Drop	0.76 ± 0.03 b				0.68 ± 0.03 b			

* Means within each column followed by the same lower-case letter are not significantly different (Tukey's HSD Test) at $p = 0.05$.

3.2. Spray Displacement Analysis

Figure 8 shows that the spray displacement for the drop nozzle was smaller compared to the no drop nozzle oriented at 0° ($F = 5.81$; $p = 0.04$; df = 1, 8). Figure 9 shows that a similar trend was evident when the nozzle was oriented at 30° ($F = 6.55$; $p = 0.03$; df = 1, 8).

When the data were combined by nozzle angle (0° and 30°) and analyzed to determine the effect of the drop vs. no drop nozzle (Figure 10), the treatments were significantly different ($F = 12.84$; $p = 0.0021$; df = 1, 18). The drop nozzle produced significantly smaller displacement than the no drop nozzle (0.18341 m vs. 0.32215 m) and accounted for a 76% reduction in displacement (Figure 11).

The regression of displacement on wind speed was upward and linear for both nozzles (Figure 11). The slope is at the rate of *b* units of Y per unit of X, where *b* is the sample regression coefficient. The following equations explained the relationship between spray displacement and wind speed for both the drop and no drop nozzles.

$$Y = 0.09451 + 0.016171 \times X; R^2 = 0.26 \text{ (Drop Nozzle)}.$$

$$Y = 0.1446 + 0.03079 \times X; R^2 = 0.19 \text{ (No Drop Nozzle)}.$$

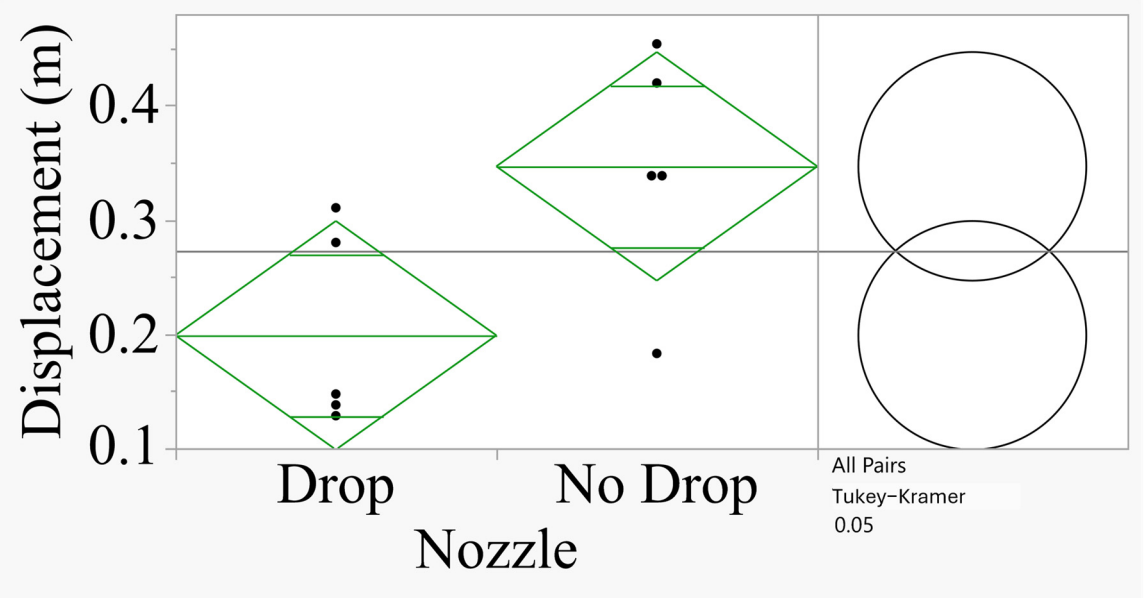

Figure 8. Analysis of spray displacement for 0° angle. The comparison circles on the right show that when the circles intersect and the angle of intersection (<90°), the means are significantly different (Tukey's HSD Test at $p = 0.05$). The black dots are individual values of displacement for each of the nozzles tested.

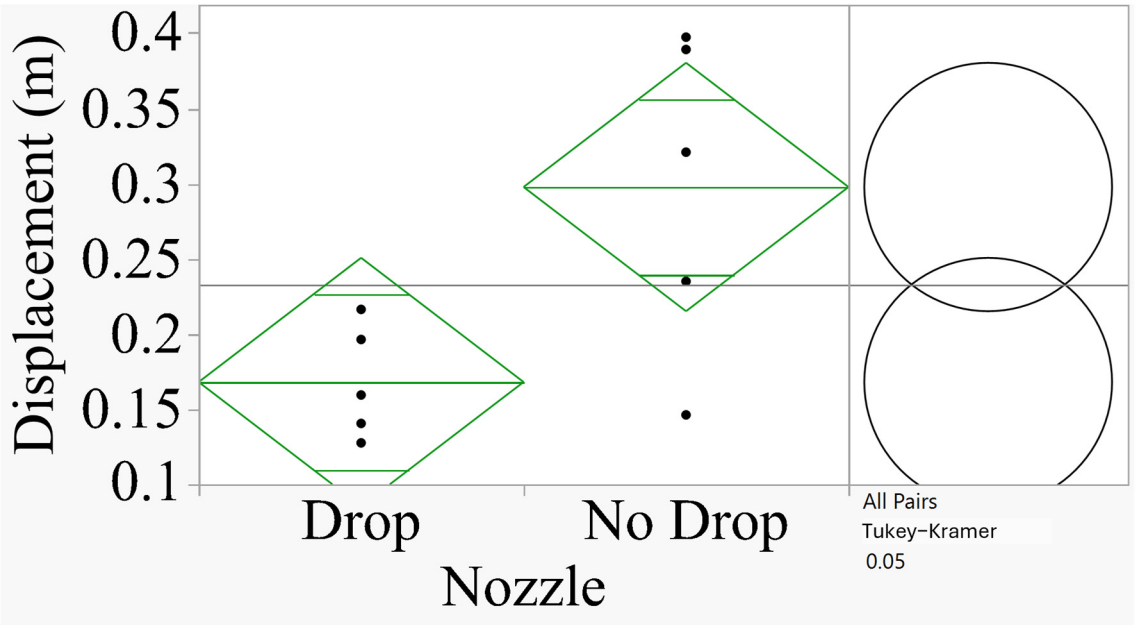

Figure 9. Analysis of spray displacement for 30° angle. The comparison circles on the right show that when the circles intersect and the angle of intersection (<90°), the means are significantly different (Tukey's HSD Test at $p = 0.05$). The black dots are individual values of displacement for each of the nozzles tested.

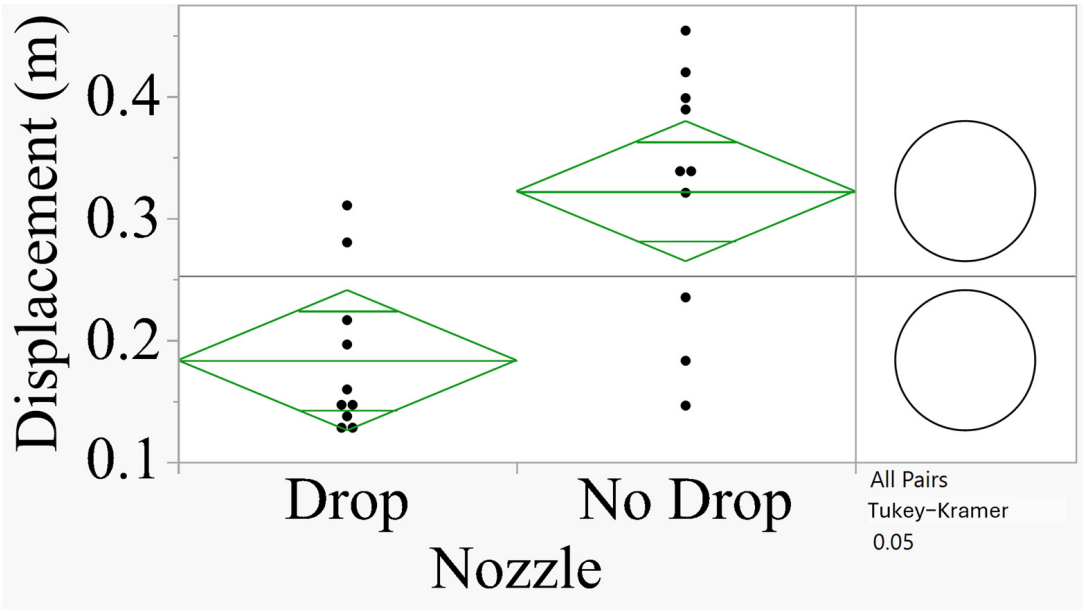

Figure 10. Relationship between spray displacement and wind speed for drop vs. no drop nozzle. The black dots are individual values of displacement for each of the nozzles tested.

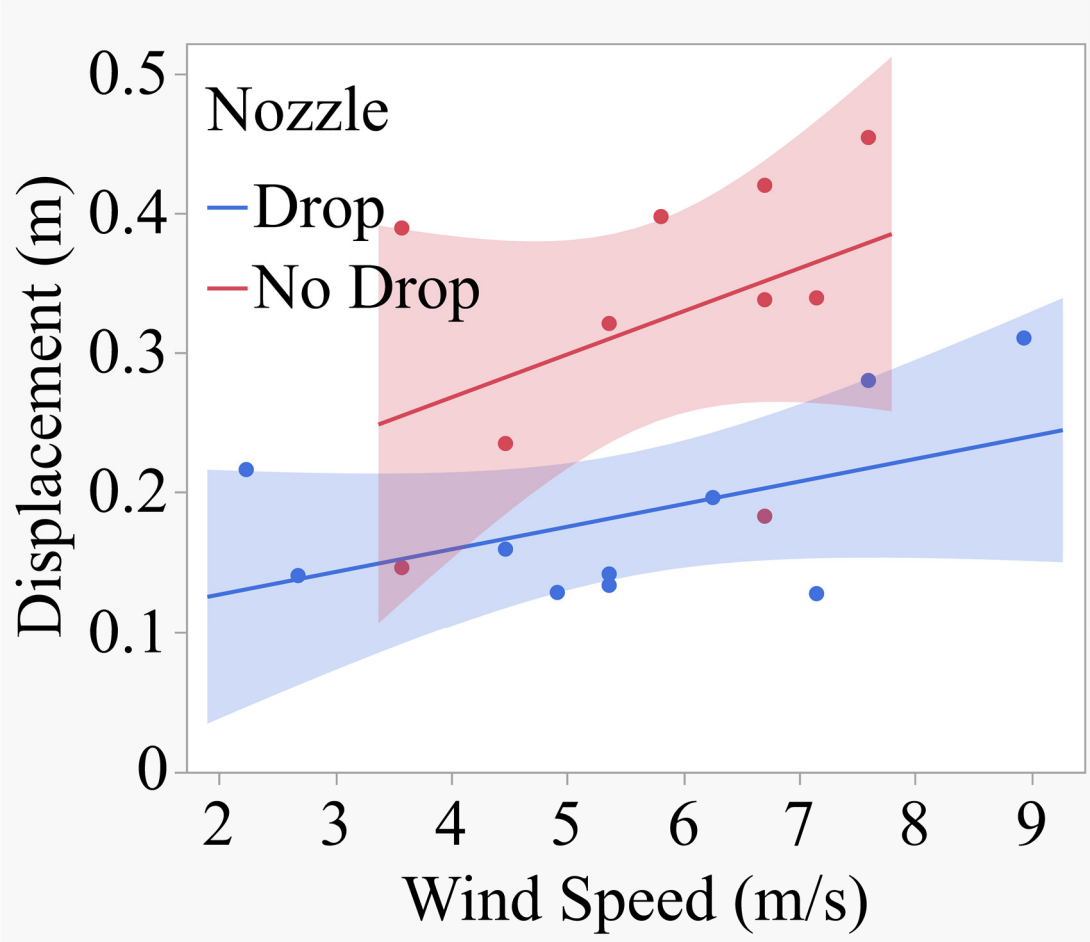

Figure 11. Relationship between spray displacement and wind speed for the drop nozzle compared to the no drop nozzle. The red and blue areas are the 95% confidence intervals for the data and the red and blue dots are the individual data points.

These equations accounted for only 26% and 19% of the variations in the model. The rate of increase in displacement for the drop nozzle was 0.01617 units for each unit increase in wind speed. Similarly, the rate of increase in displacement for the no drop nozzle was 0.03079 units for each unit increase in wind speed. The slope for the no drop nozzle was slightly higher numerically than that for the drop nozzle, and statistical differences between them could not be demonstrated. However, the drop nozzle produced significantly smaller spray displacement ($t = -3.62$; $p = 0.0023$) compared to the no drop nozzle (0.18341 m vs. 0.32215 m). The data thus indicate that the drop nozzle produced about 76% less spray displacement than the no drop nozzle. The test for the homogeneity of the regression indicated that there was no significant difference between the two slopes (Quantile = 2.12; adjusted df = 16; Adjustment = Nelson-Hsu). This suggests that the rate of spray displacement relative to wind speed was comparable between the drop and no drop nozzle and that the wind speed acted squarely for both nozzles.

3.3. Comparisons with Overall Average Decision Chart

Figure 12 shows that there was no significant difference in slopes between the drop and no drop nozzles. Both slopes are within the upper and lower confidence limits, one being above the UDL (No Drop) and the other being below the LDL (Drop).

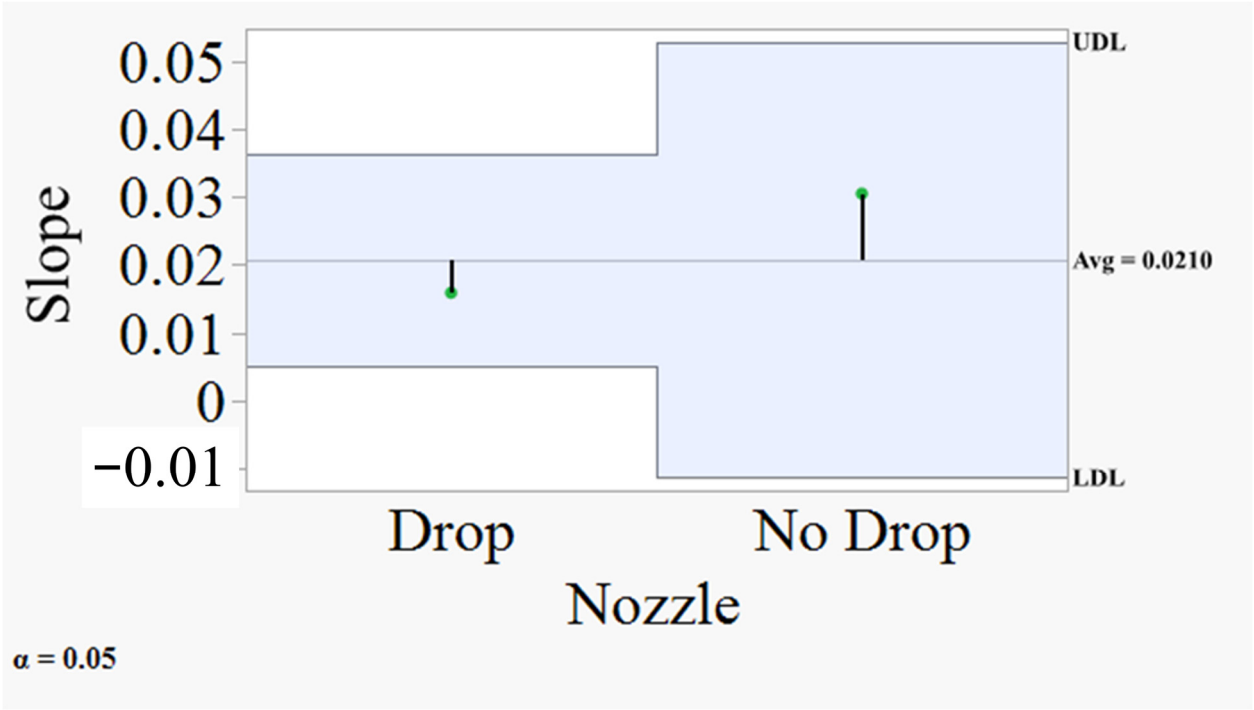

Figure 12. Comparison of slopes using ANOM Method (Quantile = 2.11991; adjusted degrees of freedom = 16; Adjustment = Nelson). The central line represents the overall average, and the treatment means plotted as deviations from the overall average are compared with lower and upper decision limits to identify which are significantly different from the overall mean. If one or more of the sample means plot outside either the upper or lower decision line, the equal means hypothesis is rejected. The drop nozzle and the no drop nozzle means (green circles) are within the decision limits and thus, the slope coefficients did not differ significantly from each other ($p = 0.05$). The green dots connected by the vertical black lines are the treatment means plotted as the deviation from the overall average.

Figure 13 shows the following equation for the 0 and 30 angle nozzles described in the relationship:

$$Y = -0.1728 + 0.06644 \times X;\ R^2 = 0.46 \text{ for the } 0^\circ \text{ nozzle.}$$

$$Y = 0.2145 + 0.004023 \times X;\ R^2 = 0 \text{ for the } 30^\circ \text{ nozzle.}$$

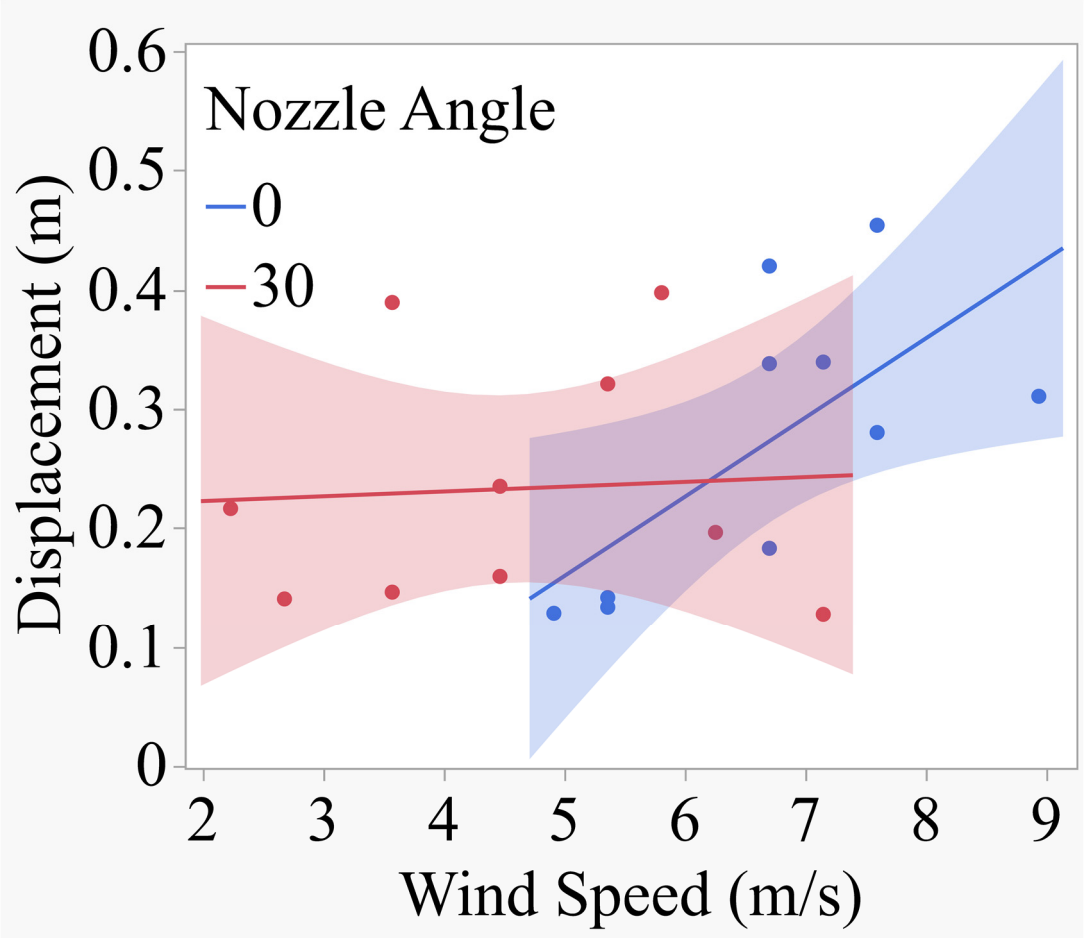

Figure 13. Regression of displacement (m) on wind speed for the 0° and 30° angle nozzles. The red and blue areas are the 95% confidence intervals for the data and the red and blue dots are the individual data points.

The slope coefficient for the 0° nozzle was significantly different from zero ($F = 6.86$; $p = 0.0307$; df = 1, 8) and suggests that displacement increased by 0.06644 m unit for every unit increase in wind speed. The slope coefficient for the 30° angle nozzle was near zero and did not vary significantly from zero ($F = 0.03$; $p = 0.8633$; df = 1, 8). It is apparent from the regression equation that displacement increased linearly with wind speed for the 0° nozzle (Figure 13). For the 30° nozzle, the regression coefficient was a flat line which indicated that the displacement did not increase with wind speed. One of the limitations of the study is that the wind speed during the test was not equal for both the nozzles. As wind speed is beyond our control, it is important that more tests should be conducted over a range of wind speeds, and replicated over time and space to obtain a better perspective on the relationship between displacement and wind speed for these nozzle angles.

4. Discussion

Zhou et al. [34] reported that the farmers in the southern United States control glyphosate resistant weeds on cotton using labor intensive methods including hand hoeing, hand spraying, spot spraying, and wick application. Recently, Unan et al. [35] reported that using a backpack sprayer, the spot spraying of clethodim herbicide applied at the labeled rate (150 g ai ha^{-1}) in a flooded rice field successfully controlled weedy rice and grasses without the dispersion of the chemical. Herbicide dispersion is a common problem in flooded rice fields, which can damage adjacent crops and have negative impacts on the species composition of non-target species, biodiversity, and reproduction. In the rice ecosystem, during the dispersion process, herbicides can spread, become immersed, and then rise to the surface where they can float or continue to float without the initial submersion [35]. Bautista et al. [36] reported that in an environmentally sensitive area in Valencia, Spain, the control of *Echinochloa* sp., a dominant weed species in rice, was achieved with the use of a RPAAS platform. Allmendinger et al. [37] reported that besides herbicide reduction, the spot spraying reduced environmental risks associated with herbicide, including herbicide leaching into the ground water, herbicide resistance development in weeds, and herbicide residues in the food chain and drift.

In this study, a significant reduction in spray displacement was observed for the drop nozzle, regardless of the nozzle angle used. This indicates that adding a 0.6 m drop tube to a spot spraying RPAAS can increase the accuracy of deposition at the wind speed that occurred during the study. Wind speed averaged 5.63 $\pm$ 0.40 m/s and varied from 2.23 to 8.94 m/s. More studies on the efficacy of drop nozzles in reducing spray displacement are warranted at various wind speeds to better understand this technology. There is little research data on the use of RPAAS platforms retrofitted with drop nozzles vis-à-vis spray displacement under field conditions where the vagaries of weather predominate. Allmendinger et al. [37] reported on commercially available spot spraying systems comprising sensors and classifiers for weed detection and decision algorithms to decide whether weed control is needed. A survey conducted on farmers in the southern United States indicated that resistant weed control on cotton was performed using labor intensive techniques and that no education programs on better weed management technique were developed to help the farmers.

Between the four treatments, a wide range of coverage was achieved on the target site. Due to using Kromekote cards instead of plant material as the target, the potential for spray coverage seems to be higher than expected. When looking at what coverage is required for herbicide efficacy, it largely depends on the type of plant and herbicide being used. Expected normal values were established by Hunter et al. [38] as 30–60% when using an unmanned aerial sprayer with a conventional broadcast boom. Between systemic and contact herbicides, it was found that systemic have a lower coverage requirement, with coverage as low as 18.96% being sufficient. However, contact herbicides required significantly higher coverage with 41.67% being the lowest coverage found to be effective [39]. The values presented, while being a starting point, are not guaranteed to be effective in all situations. The nozzles used in this study all provided a level of coverage sufficient to meet the minimum coverage as suggested by Prokop [39].

Limitations present during the study included, wind not being consistent between all trials. This means that trials are not perfectly identical in terms of environmental conditions, which could potentially introduce error in the distribution of the data. Other limitations included using Kromekote cards instead of plants as the target, and being limited to constant nozzle height or constant RPAAS height. By using cards instead of plants, the movement of the leaves by rotor wash, which is a major factor in aerial applications, is mitigated. The last limitation in the study was being restricted to testing only different

nozzle heights or RPAAS heights. For this study, RPAAS height was chosen as a constant. This allowed for the drop nozzle to be tested without changing any flight parameters from a conventional spot spraying application.

A crucial next step in researching spot spraying with RPAAS is to investigate the effects of rotor wash on spray droplets to determine whether they reach the intended target area. The characteristics of rotor wash can vary greatly between each RPASS due to the factory-installed configurations of these platforms. While several studies have examined the impact of rotor wash on a multi-rotor RPAAS platforms [40–43], few such data exist for spray drones configured for spot spraying. The down-wash air flow generated by rotor wings can significantly influence deposition, penetration, distribution, and swath width of the RPAAS platforms. The air flow could also help the penetration of the spray droplets into the lower canopy [40–42]. Richarson et al. [23] reported that for conventional aerial spraying, deposition is measured along the sampling line perpendicular to the direction of the flight, while for spot spraying, the deposition pattern is two-dimensional. These data warrant further investigation. Asghadi et al. [44] demonstrated that a custom-designed robotic spot spraying system installed on a RPAAS vehicle effectively controlled grassy weeds in a sugarcane farm, and that it reduced the concentration of herbicides in runoff water as much as 39% compared to broadcast spraying. Although these developments are exciting, whether the robotic spraying system will become practical for use by farmers in fields awaits many years of research.

5. Conclusions

The drop nozzle system used in this study was improvised and outfitted to the RPAAS platform to perform spot spraying of resistant weeds, which normally occur in a clumped distribution pattern. Results indicate that a drop nozzle with a straight stream or 30° cone nozzle can minimize spray displacement and facilitate more precise placement of herbicides on desired weed species. The drop nozzle produced significantly smaller spray displacement compared to the no drop nozzle (0.183 vs. 0.322 m), and indicates that the drop nozzle produced about 76% lower spray displacement than the no drop nozzle. The test for the homogeneity of the regression indicated that there was no significant difference between the two slopes. This suggests that the rate of spray displacement relative to wind speed prevalent at the time of this study was comparable between the drop and no drop nozzle. The relative span (RS) was significantly narrower for both the 0° ($\overline{x} = 0.76 \pm 0.03$) and 30° ($\overline{x} = 0.68 \pm 0.03$) angled no drop nozzles compared to the drop nozzles ($\overline{x} = 0.85 \pm 0.02$ for 0°and $\overline{x} = 0.87 \pm 0.03$ for 30°). This suggests that the smaller, more driftable fractions of the spray ($D_{v0.1}$, µm) did not deposit on the targeted area for the no drop nozzle. Thus, it would reduce the RS, which is based on the difference between $D_{v0.9}$ and $D_{v0.1}$ divided by $D_{v0.5}$. When a smaller droplet fraction is blown away from the target, the $D_{v0.1}$ value increases, thus making the difference between $D_{v0.9}$ and $D_{v0.1}$ smaller, which reduces the RS.

This study shows that the technique of using drop nozzles for the control of resistant weeds can help minimize the off-target movement of hazardous chemicals and mitigate spray drift. The potential to increase farm productivity by reducing input costs makes this method of chemical application a viable alternative to current spot spraying methods. This study has shown that wind speed was twice as high when the 0° angle nozzle was tested compared to the 30° angle nozzle test. Thus, additional research evaluating the accuracy and efficacy of herbicide applications under various meteorological conditions should develop our understanding of spot spraying technology for resistant weed control.

Author Contributions: Conceptualization, D.E.M. and S.A.N.; methodology, D.E.M.; software, R.P.G.; validation, R.P.G. and Z.S.H.; formal analysis, R.P.G.; resources, D.E.M. and M.A.L.; writing—original draft preparation, R.P.G.; writing—review and editing, R.P.G., D.E.M., Z.S.H., S.A.N. and M.A.L.; visualization, R.P.G. All authors have read and agreed to the published version of the manuscript.

Funding: This research received no external funding.

Data Availability Statement: The original contributions presented in this study are included in the article. Further inquiries can be directed to the corresponding author.

Conflicts of Interest: The authors declare no conflicts of interest. This research received no external funding. The use of trade, firm or corporation names in this publication is for the information and convenience of the reader. Such use does not constitute an official endorsement or approval by the United States Department of Agriculture or the Agricultural Research Service of any product or service to the exclusion of others that may be suitable.

References

1. Soltani, N.; Dille, J.A.; Burke, I.C.; Everman, W.J.; VanGessel, M.J.; Davis, V.M.; Sikkema, P.H. Potential corn yield losses from weeds in North America. *Weed Technol.* **2016**, *30*, 979–984. [CrossRef]
2. James, T.; Rahman, A.; Mellsop, J. Weed competition in maize crop under different timings for postemergence weed control. *N. Z. Plant Prot.* **2000**, *53*, 269–272. Available online: http://www.nzpps.org/terms_of_use.html (accessed on 10 December 2024). [CrossRef]
3. Sardana, V.; Mahajan, G.; Jabran, K.; Chauhan, B.S. Role of competition in managing weeds: An introduction to the special issue. *Crop Protect.* **2017**, *95*, 1–7. [CrossRef]
4. Fernando, N.; Manalil, S.; Florentine, S.K.; Chauhan, B.S.; Seneweera, S. Glyphosate resistance of C3 and C4 weeds under rising atmospheric CO_2. *Front. Plant Sci.* **2016**, *7*, 910. [CrossRef] [PubMed]
5. Kaur, R.; Kumar, S.; Ali, S.; Kumar, S.; Ezing, U.; Bana, R.; Meena, S.; Dass, A.; Singh, T. Impacts of climate change on crop-weed dynamics: Challenges and strategies for weed management in a changing climate. *J. Environ. Biol.* **2024**, *9*, 015–021.
6. Amare, T. Review on impact of climate change on weed and their management. *Amer. J. Biol. Environ. Stat.* **2016**, *2*, 21–27. [CrossRef]
7. Baldwin, F.L. Transgenic crops: A view from the US Extension Service. *Pest Manag. Sci.* **2000**, *56*, 584–585. [CrossRef]
8. Johnson, G.A.; Mortensen, D.A.; Gotway, C.A. Spatial and temporal analysis of weed seedling populations using geostatistics. *Weed Sci.* **1996**, *44*, 704–710. [CrossRef]
9. Nobre, F.L.d.L.; Santos, R.F.; Herrera, J.L.; Araújo, A.L.d.; Johann, J.A.; Gurgacz, F.; Siqueira, J.A.C.; Prior, M. Use of drones in herbicide spot spraying: A systematic review. *Adv. Weed Sci.* **2024**, *41*, e020230014. [CrossRef]
10. Sétamou, M.; Bartels, D.W. Living on the edges: Spatial niche occupation of Asian citrus psyllid, *Diaphorina citri* Kuwayama (Hemiptera: Liviidae), in citrus groves. *PLoS ONE* **2015**, *10*, e0131917. [CrossRef] [PubMed]
11. Severtson, D.; Flower, K.; Nansen, C. Nonrandom distribution of cabbage aphids (Hemiptera: Aphididae) in dryland canola (Brassicales: Brassicaceae). *Environ. Entomol.* **2015**, *44*, 767–779. [CrossRef] [PubMed]
12. Nguyen, H.D.D.; Nansen, C. Edge-biased distributions of insects. A review. *Agron. Sustain. Dev.* **2018**, *38*, 11. [CrossRef]
13. Mattson, W.J.; Haack, R.A. The role of drought in outbreaks of plant-eating insects. *Bioscience* **1987**, *37*, 110–118. Available online: https://www.jstor.org/stable/1310365 (accessed on 10 December 2024). [CrossRef]
14. Walter, A.J.; Difonzo, C.D. Soil potassium deficiency affects soybean phloem nitrogen and soybean aphid populations. *Environ. Entomol.* **2014**, *36*, 26–33. [CrossRef]
15. West, K.; Nansen, C. Smart-use of fertilizers to manage spider mites (Acari: Tetrachynidae) and other arthropod pests. *Plant Sci. Today* **2014**, *1*, 161–164. [CrossRef]
16. Lillesand, T.; Kiefer, R.W.; Chipman, J. *Remote Sensing and Image Interpretation*; John Wiley & Sons: Hoboken, NJ, USA, 2015.
17. Torres-Sánchez, J.; López-Granados, F.; De Castro, A.I.; Peña-Barragán, J.M. Configuration and specifications of an unmanned aerial vehicle (UAV) for early site specific weed management. *PLoS ONE* **2013**, *8*, e58210. [CrossRef]
18. Abbasi, R.; Martinez, P.; Ahmad, R. The digitization of agricultural industry—A systematic literature review on agriculture 4.0. *Smart Agric. Technol.* **2022**, *2*, 100042. [CrossRef]
19. Hunter III, J.E.; Gannon, T.W.; Richardson, R.J.; Yelverton, F.H.; Leon, R.G. Integration of remote-weed mapping and an autonomous spraying unmanned aerial vehicle for site-specific weed management. *Pest Manag. Sci.* **2020**, *76*, 1386–1392. [CrossRef]
20. Zhang, C.; Kovacs, J.M. The application of small unmanned aerial systems for precision agriculture: A review. *Precis. Agric.* **2012**, *13*, 693–712. [CrossRef]

21. Xiang, H.; Tian, L. Development of a low-cost agricultural remote sensing system based on an autonomous unmanned aerial vehicle (UAV). *Biosys. Eng.* **2011**, *108*, 174–190. [CrossRef]
22. Allmendinger, A.; Spaeth, M.; Saile, M.; Peteinatos, G.G.; Gerhards, R. Agronomic and Technical Evaluation of Herbicide Spot Spraying in Maize Based on High-Resolution Aerial Weed Maps—An On-Farm Trial. *Plants* **2024**, *13*, 2164. [CrossRef]
23. Richardson, B.; Rolando, C.A.; Kimberley, M.O. Quantifying spray deposition from a UAV configured for spot spray applications to individual plants. *Trans. ASABE* **2020**, *63*, 1049–1058. [CrossRef]
24. Singh, V.; Rana, A.; Bishop, M.; Filippi, A.M.; Cope, D.; Rajan, N.; Bagavathiannan, M. Unmanned aircraft systems for precision weed detection and management: Prospects and challenges. *Adv. Agron.* **2020**, *159*, 93–134. [CrossRef]
25. Roslim, M.H.M.; Juraimi, A.S.; Che'Ya, N.N.; Sulaiman, N.; Manaf, M.N.H.A.; Ramli, Z.; Motmainna, M. Using remote sensing and an unmanned aerial system for weed management in agricultural crops: A review. *Agronomy* **2021**, *11*, 1809. [CrossRef]
26. Ghatrehsamani, S.; Jha, G.; Dutta, W.; Molaei, F.; Nazrul, F.; Fortin, M.; Bansal, S.; Debangshi, U.; Neupane, J. Artificial intelligence tools and techniques to combat herbicide resistant weeds—A review. *Sustainability* **2023**, *15*, 1843. [CrossRef]
27. Delbert, C. This Badass Robot Uses Lasers to Slay 100,000 Weeds per Hour. 2021. Available online: https://www.popularmechanics.com/technology/robots/a36331690/autonomous-farming-robot-kills-weeds/ (accessed on 6 January 2025).
28. Bradley, K. Weed Electrocution Research Sparks Interest as Herbicide Resistance Impedes Current Methods. 2021. Available online: https://extension.missouri.edu/news/weed-electrocution-research-sparks-interest-as-herbicide-resistance-impedes-current-methods (accessed on 6 January 2025).
29. Python Software Foundation. *Anaconda Software*, Version 2-2.4.0; Python Software Foundation: Wilmington, DE, USA, 2024.
30. ASABE. *Spray Nozzle Classification by Droplet Spectra*; ANSI/ASAE S572.3; ASABE: St. Joseph, MI, USA, 2020.
31. SAS. *JMP® 14*; SAS Institute Inc.: Cary, NC, USA, 2018.
32. Snedecor, G.W.; Cochran, W.G. *Statistical Methods*, 6th ed.; The Iowa State University Press: Ames, IA, USA, 1967; p. 593.
33. SAS Institute. *SAS/QC® 14.1 User's Guide The ANOM Procedure*; 14.1; SAS Institute Inc.: Cary, NC, USA, 2015.
34. Zhou, X.; Roberts, R.K.; Larson, J.A.; Lambert, D.M.; English, B.C.; Mishra, A.K.; Falconer, L.L.; Hogan Jr, R.J.; Johnson, J.L.; Reeves, J.M. Differences in glyphosate-resistant weed management practices over time and regions. *Weed Technol.* **2016**, *30*, 1–12. [CrossRef]
35. Unan, R.; Galvin, L.; Becerra-Alvarez, A.; Al-Khatib, K. Assessing clethodim spot spraying applications for control of problematic weedy rice and other grasses in California rice fields. *Agron. J.* **2024**, *116*, 302–312. [CrossRef]
36. Bautista, A.S.; Tarrazó-Serrano, D.; Uris, A.; Blesa, M.; Estruch-Guitart, V.; Castiñeira-Ibáñez, S.; Rubio, C. Remote Sensing Evaluation Drone Herbicide Application Effectiveness for Controlling *Echinochloa* spp. in Rice Crop in Valencia (Spain). *Sensors* **2024**, *24*, 804. [CrossRef] [PubMed]
37. Allmendinger, A.; Spaeth, M.; Saile, M.; Peteinatos, G.G.; Gerhards, R. Precision chemical weed management strategies: A review and a design of a new CNN-based modular spot sprayer. *Agronomy* **2022**, *12*, 1620. [CrossRef]
38. Hunter, J.E., III. Integration of Unmanned Aerial Vehicles (UAVs) for Remote Sensing and Spray Applications for Weed Management. Ph.D. Thesis, North Carolina State University, Raleigh, NC, USA, 2019.
39. Prokop, M. Leaves coverage of spray liquid and influence on herbicide efficacy. *Acta Univ. Agric. Silvic. Mendel. Brun.* **2009**, *57*, 263–270. [CrossRef]
40. Coombes, M.; Newton, S.; Knowles, J.; Garmory, A. The influence of rotor downwash on spray distribution under a quadrotor unmanned aerial system. *Comput. Electron. Agric.* **2022**, *196*, 106807. [CrossRef]
41. Zhang, H.; Lan, Y.; Shen, N.; Wu, J.; Wang, T.; Han, J.; Wen, S. Numerical analysis of downwash flow field from quad-rotor unmanned aerial vehicles. *Inter. J. Precis. Agric. Aviat.* **2020**, *3*, 1–7. [CrossRef]
42. Yang, Z.; Qi, L.; Wu, Y. Influence of UAV Rotor Down-wash Airflow For Droplet Penetration. In Proceedings of the 2018 ASABE Annual International Meeting, Detroit, MI, USA, 29 July–1 August 2018. [CrossRef]
43. Tan, Y.; Chen, J.; Norton, T.; Wang, J.; Liu, X.; Yang, S.; Zheng, Y. The computational fluid dynamic modeling of downwash flow field for a six-rotor UAV. *Front. Agric. Sci. Eng.* **2018**, *5*, 159–167. [CrossRef]
44. Azghadi, M.R.; Olsen, A.; Wood, J.; Saleh, A.; Calvert, B.; Granshaw, T.; Fillols, E.; Philippa, B. Precise robotic weed spot-spraying for reduced herbicide usage and improved environmental outcomes—A real-world case study. *arXiv* **2024**, arXiv:2401.13931. [CrossRef]